Hanle electromagnetically induced transparency and absorption resonances with a Laguerre Gaussian beam

J. Anupriya, Nibedita Ram, and M. Pattabiraman*
Department of Physics, Indian Institute of Technology, Madras, Chennai 600036, India
(Received 11 November 2009; published 5 April 2010)

We describe a computational and experimental study on Hanle electromagnetically induced transparency and absorption resonance line shapes with a Laguerre Gaussian (LG) beam. It is seen that the LG beam profile brings about a significant narrowing in the line shape of the Hanle resonance and ground-state Zeeman coherence in comparison to a Gaussian beam. This narrowing is attributed to the azimuthal mode index of the LG field.

DOI: 10.1103/PhysRevA.81.043804 PACS number(s): 42.50.Gy, 32.80.Qk, 32.70.Jz

I. INTRODUCTION

The interaction of a coherent laser light with an atomic system induces coherence among the energy levels of the system. Atomic wave functions with a definite phase relation among them are then created resulting in interference phenomenon. This is referred to as atomic coherence and has lead to interesting effects such as coherent population trapping (CPT), electromagnetically induced transparency or absorption (EIT or EIA) and the Hanle effect [1–3]. EIT is a phenomenon in which the atomic medium is rendered transparent for a resonant probe field in the presence of another pump beam resonant with a common higher or lower energy level. The underlying principle behind EIT can be explained in terms of the creation of dark states, that is, the uncoupled state which comprises the superposition of the ground states. Destructive interference between the probability amplitude associated with the excitation pathways can be brought about by adjusting the Rabi frequency associated with the probe and the pump beam, thus totally cutting off the dark state from coupling to the higher energy level. This results in the trapping of atoms in the dark state thus making the medium transparent to the probe absorption [4,5].

EIA is an opposite effect in which there is an enhancement in probe absorption under the action of a pump beam due to the transfer of coherence between the excited and ground states via spontaneous emission in a two-level degenerate system [6,7]. EIT and EIA in a degenerate two-level system can also be observed in the Hanle configuration, by measuring the transmission or fluorescence of a resonant optical field as a function of a magnetic field scanned through zero [8]. The narrow Hanle EIT-EIA profile arises as a result of the destruction of optical-field-induced coherence among ground- or excited-state Zeeman sublevels by a magnetic field [9].

In this report we focus on such Zeeman coherences created in the presence of a coherent light with spatially varying phase factor and mode amplitude. The Laguerre-Gaussian (LG) beam is one such optical field with a doughnut-shaped intensity distribution and zero intensity at the beam center [10]. It is obtained as a solution of the paraxial wave function in cylindrical coordinates. The LG beam has several interesting features. It has a helical phase structure [10] and carries an orbital angular momentum of $l\hbar$ per photon along their direction of propagation, in addition to the spin angular momentum depending upon the polarization ($l = \pm 1, \pm 2, \ldots$ is the azimuthal mode index and denotes order of the LG beam).

The optical forces and torque exerted by the LG beam on particles and atoms have been studied extensively and they find interesting applications in cooling and trapping of atoms [10–12]. Nonlinear optical studies like the second harmonic generation with higher order LG beams have been reported [13]. The rotational frequency shifts induced by the LG beam due to its azimuthal phase dependence have been observed [14–16]. Theoretical studies of force and mechanical torque exerted by orbital angular momentum associated with the LG beam on two- and three-level atomic systems have also been reported [11,17,18].

The influence of the LG beam profile on atomic coherence and associated spectroscopic phenomenon like EIT and EIA, Hanle effect, etc. is however not well known. In this paper we focus on this aspect and report a computational and experimental study of the Hanle EIA and EIT line shapes obtained with an LG beam. We report for the first time a significant narrowing of the LG Hanle line shape and the associated Zeeman coherence compared to the profile obtained with a Gaussian beam and show that it arises due to the nonzero azimuthal mode index of the LG field resulting in a spatially dependent Rabi frequency.

II. THEORETICAL MODEL

The field amplitude, E_{LG} for the LG mode is defined in terms of mode amplitude $\varepsilon_{\mathrm{klp}}(\mathbf{R})$ and the phase factor $\theta_{\mathrm{klp}}(\mathbf{R})$ as [11,18]

$$E_{\mathrm{LG}} = \varepsilon_{\mathrm{klp}}(\mathbf{R})\, e^{\mathrm{i}\Theta_{\mathrm{klp}}(\mathbf{R})} - \text{c.c.}, \tag{1}$$

where k is the wave vector, p is the radial mode index, and c.c. denotes the complex conjugate of the first term in the right-hand side of Eq. (1). Ignoring the z dependence in the region $z \ll$ Rayleigh length '$z_{\mathbf{R}}$' [11] and making the dipole approximation, E_{LG} reduces to

$$E_{\mathrm{LG}} \approx E^{o}_{\mathrm{LG}} \left(\frac{r}{w(z)}\right)^{|l|} e^{-\frac{r^2}{w(z)^2}} e^{-il\phi} - \text{c.c.}, \tag{2}$$

*pattu@physics.iitm.ac.in

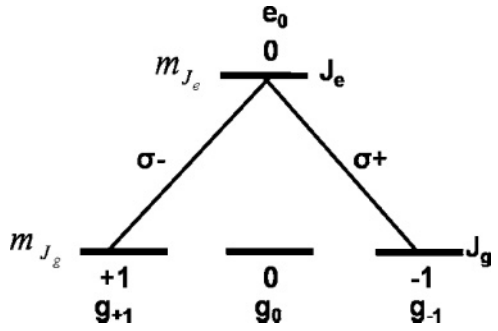

FIG. 1. Atomic level configuration for the transition $J_g = 1 \rightarrow J_e = 0$.

where $e^{-il\phi}$ is the phase factor and its coefficient represents the reduced mode amplitude of the electric field.

To study the effect of the LG field on the Hanle line shape, the transition $J_g = 1 \rightarrow J_e = 0$ (Fig. 1) was chosen, where J_g and J_e represent the total angular momentum quantum number of the ground and excited states, respectively. This system produces a well-known Hanle EIT [19]. We consider a σ polarized probe beam $[(\sigma^+ + \sigma^-)/2]$ which accesses transitions satisfying the selection rule $\Delta m_j = \pm 1$. The total Hamiltonian H of the system is given by the sum of the unperturbed Hamiltonian H_o, the atom-field interaction Hamiltonian H_I, and the magnetic interaction energy H_B,

$$H_o = \sum_i \hbar\omega_{g_i} |g_i\rangle \langle g_i| + \sum_i \hbar\omega_{e_i} |e_i\rangle \langle e_i| \tag{3}$$

$$H_I = \sum_{\substack{i,j \\ i\neq j}} |i\rangle \langle j| \{(d_{ij}.\vec{E})_{\sigma+} + (d_{ij}.\vec{E})_{\sigma-}\} + \text{H.c.} \tag{4}$$

$$H_B = \sum_{i\neq 0} \Omega_L \{m_{g_i} |g_i\rangle \langle g_i| + m_{e_i} |e_i\rangle \langle e_i|\}, \tag{5}$$

where H.c. is the Hermitian conjugate of the first term in Eq. (4). The Larmor frequency $\omega_L = \frac{g\mu_B B}{\hbar}$, where B is the magnetic field, μ_B is the Bohr magneton, and g the gyromagnetic ratio. The magnetic field direction was chosen perpendicular to both the optical field propagation and polarization directions. The quantization axis was chosen along the magnetic field direction. The electric field vector associated with the probe beam propagating along the z direction and polarized in the x direction is given by

$$\vec{E} = E_o \cos(\omega t)\, \hat{e}_x. \tag{6}$$

For a Gaussian beam E_o is taken as a constant, and for a LG beam E_o is replaced by E_{LG} (Eq. (2)). The dipole matrix element d_{ij} is given by [20]

$$d_{ij} = e\langle \alpha_e J_e || r || \alpha_g J_g \rangle (-1)^{J_e - m_e} \begin{pmatrix} J_e & 1 & J_g \\ -m_e & q & m_g \end{pmatrix},$$

where the angled brackets denote the reduced matrix element and the term in parenthesis is a 3-j symbol. The Rabi frequencies associated with the Gaussian and LG modes are given by

$$\mathbf{\Omega}_G = \frac{d_{ij} E_o}{\hbar} \tag{7}$$

$$\mathbf{\Omega}_{\text{LG}} = \frac{d_{ij} E_{\text{LG}}}{\hbar} = \mathbf{\Omega}^o_{\text{LG}} \left(\frac{r}{w(z)}\right)^{|l|} e^{-\frac{r^2}{w(z)^2}} e^{-il\phi}, \tag{8}$$

where, $\mathbf{\Omega}^o_{\text{LG}} = \frac{d_{ij} E^o_{\text{LG}}}{\hbar}$. Here, $w(z)$ represents the beam waist for a beam width of w_o and is given by [10] $w(z) = w_o\sqrt{1 + (z/z_R)^2} \approx w_o$ for $z \ll z_R$. The time evolution of the density matrix ρ is given by the Liouville equation [21],

$$\frac{d\rho}{dt} = \frac{i}{\hbar}[\rho, \tilde{H}] - \frac{1}{2}\{\tilde{R}, \rho\} + \Lambda_\Gamma + \Lambda_\Upsilon, \tag{9}$$

where $\tilde{H}$ is the total Hamiltonian of the system after making the rotating wave approximation [22]. The first and the second terms on the right-hand side of Eq. (9) represent the commutation and anticommutation operations, respectively. $\tilde{R}$ is the relaxation operator comprising the spontaneous decay rate, Γ of the excited state, the ground-state collisional decay rate γ_g, and the excited-state collisional decay rate γ_e (with $\gamma_e = \gamma_g = \gamma$). The effects of collisional dephasing are not included here. Λ_Γ and Λ_γ denote the re-population matrix of the ground state due to the relaxation terms Γ and γ, respectively.

The optical Bloch equations (OBE) obtained from Eq. (9) are numerically solved [23] under steady-state conditions by setting the right-hand side of (9) to zero. The steady-state probe absorption α is given by [24]

$$\alpha = \sum_{\substack{i,j \\ i\neq j}} \frac{2\sqrt{2}\pi\boldsymbol{\omega}_o N}{\hbar c \mathbf{\Omega}} |d_{ij}|^2 \begin{pmatrix} J_e & 1 & J_g \\ -m_e & q & m_g \end{pmatrix} \text{Im}\left[\rho_{e_i}\rho_{g_j}\right], \tag{10}$$

where $\boldsymbol{\omega}_o$ is the frequency difference between the ground and the excited states in the absence of the magnetic field and N is the density of atoms. For a Gaussian beam, Eq. (10) is used to compute the absorption with the Rabi frequency $\Omega(=\Omega_G)$, treated as a constant.

To compute the probe absorption for the LG beam, $\mathbf{\Omega}$ in Eq. (10) is replaced by $\mathbf{\Omega}_{\text{LG}}$ (with $\mathbf{\Omega}^o_{\text{LG}}$ treated as a constant) and a double integration carried out over parameters r and ϕ [ignoring the z dependence as in Eq. (2)],

$$\alpha_{\text{LG}} = \int_{r=0}^{w_o} \int_{\phi=0}^{2\pi} \sum_{\substack{i,j \\ i\neq j}} \frac{2\sqrt{2}\pi\mathbf{\Omega}_o N}{\hbar c \mathbf{\Omega}^o_{\text{LG}} \left(\frac{r}{w(z)}\right)^{|l|} e^{-\frac{r^2}{w(z)^2}} e^{-il\phi}} \times |d_{ij}|^2 \begin{pmatrix} J_e & 1 & J_g \\ -m_e & q & m_g \end{pmatrix} \text{Im}\left[\rho_{e_i}\rho_{g_j}\right] dr d\phi. \tag{11}$$

III. COMPUTATIONAL RESULTS

The calculated absorption of the incident optical field as a function of magnetic field (the Hanle profile) for Gaussian and LG beams is shown in Fig. 2. The azimuthal mode index associated with the LG beam is taken as $l = +1$ with $\Gamma/\gamma = 20$, $\mathbf{\Omega}^{\text{LG}}_o/\Gamma = 1$, $\mathbf{\Omega}_G/\Gamma = 1$, and $w(z) \approx w_0 = 2\,\text{mm}$. The LG Hanle profile is significantly narrower than the one that is obtained with the Gaussian beam. The computed

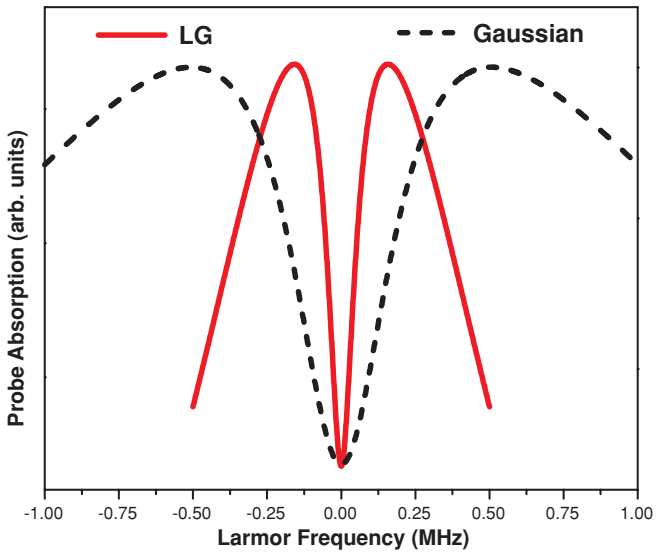

FIG. 2. (Color online) Calculated Hanle resonance for $J_g = 1 \rightarrow J_e = 0$ with Gaussian and LG fields using $\Gamma/\gamma = 20$, $\mathbf{\Omega}_o^{\mathrm{LG}}/\Gamma = 1$, $\mathbf{\Omega}_G/\Gamma = 1$, and $w_o = 2\,\mathrm{mm}$ for $l = +1$. The absorption-axis scales for Gaussian and LG profiles were chosen differently to aid linewidth comparison of the EIT windows. The absorption profile with LG field has been scaled by a multiplicative factor of 6.

Hanle profile linewidths for the Gaussian and LG beams are 0.363 MHz and 0.105 MHz, respectively. The ground-state Zeeman coherence $\rho_{g_{-1}g_{+1}}$—responsible for the Hanle EIT resonance [25]—computed by integrating over parameters r and ϕ also exhibits a similar narrowing as shown in Fig. 3.

The source of the narrowing in the computation originates in the presence of the spatially dependent Rabi frequency [Eq. (8)] in the interaction Hamiltonian [Eq. (4)] and in the Liouville equation [(Eq. (9)]. To understand the origin of this narrowing, we recomputed the probe absorption and Zeeman coherence with $\mathbf{\Omega}_{\mathrm{LG}} \approx \mathbf{\Omega}_o^{\mathrm{LG}} e^{-il\phi}$, ignoring the radial

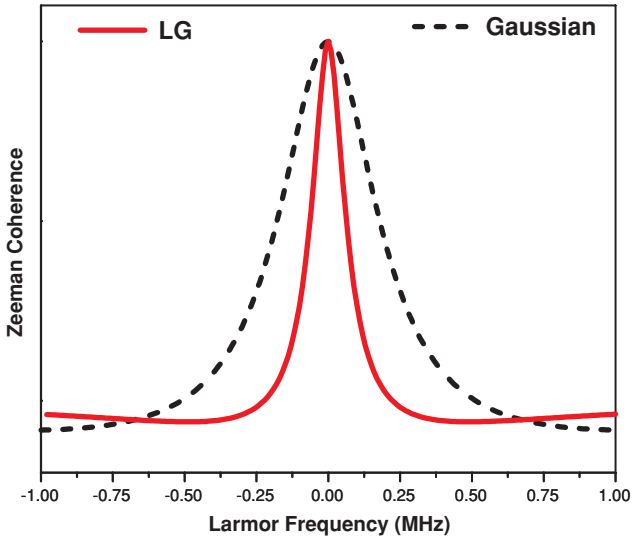

FIG. 3. (Color online) Normalized ground-state Zeeman coherence created by Gaussian and LG fields. Parameters are the same as those used in Fig. 2.

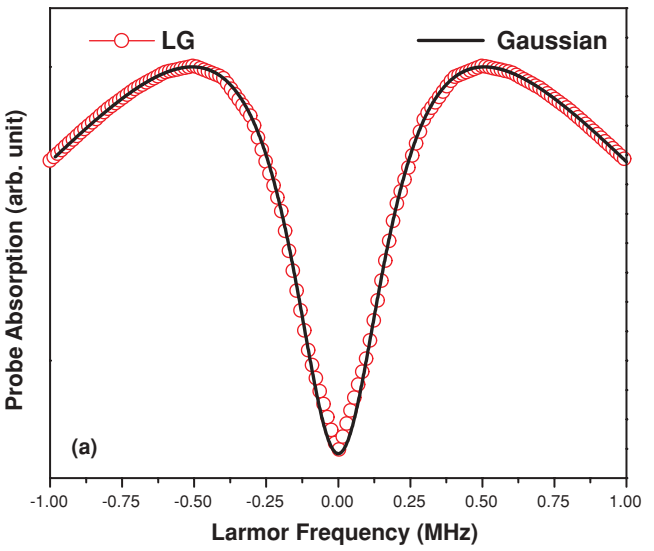

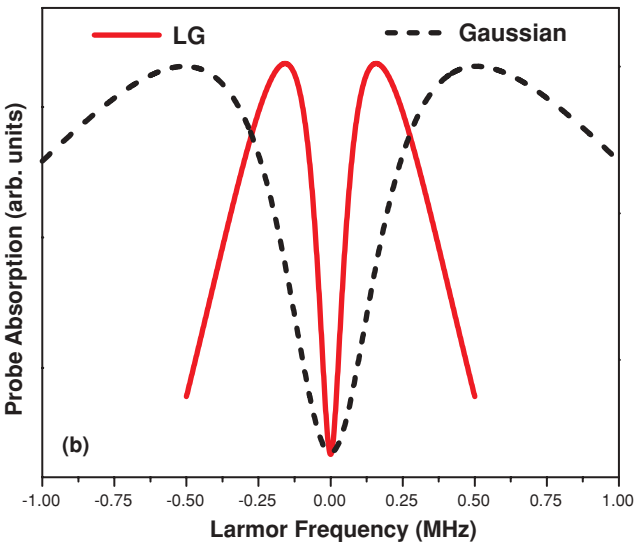

FIG. 4. (Color online) Probe absorption for $J_g = 1 \rightarrow J_e = 0$ due to Gaussian and LG beams. In (a) the radial dependence of $\mathbf{\Omega}_{\mathrm{LG}}$ has been ignored and in (b) the phase factor in $\mathbf{\Omega}_{\mathrm{LG}}$ has been ignored. Other parameters are same as those used in Fig. 2. See text for details.

dependence. It is seen from Fig. 4(a) that the narrowing is absent. Alternatively, if the phase factor is ignored, $\mathbf{\Omega}_{\mathrm{LG}} \approx \mathbf{\Omega}_{\mathrm{LG}}^{o}[r/w(z)]^{|l|} \exp[-r^2/w(z)^2]$, the same narrowing is observed in the Hanle profile [Fig. 4(b)] and the Zeeman coherence. The reduced mode amplitude of the electric field associated with the LG beam reduces to the far field intensity of a Gaussian beam when $l = 0$. This suggests that the azimuthal mode index (l) associated with the LG beam which features in $\mathbf{\Omega}_{\mathrm{LG}}$ brings about the observed narrowing.

The Hanle signal linewidth is determined by the relaxation rate of ground- or excited-state Zeeman coherences [3]. Therefore a narrow Hanle signal suggests that an optical field with nonzero orbital angular momentum ($l\hbar$) promotes long-lived Zeeman coherences. Further support for this possibility is found when the Hanle profile with the LG field was computed for different azimuthal mode indices $l = +1, +2$, and $+3$ with beam waists chosen as 2 mm, 3 mm, and

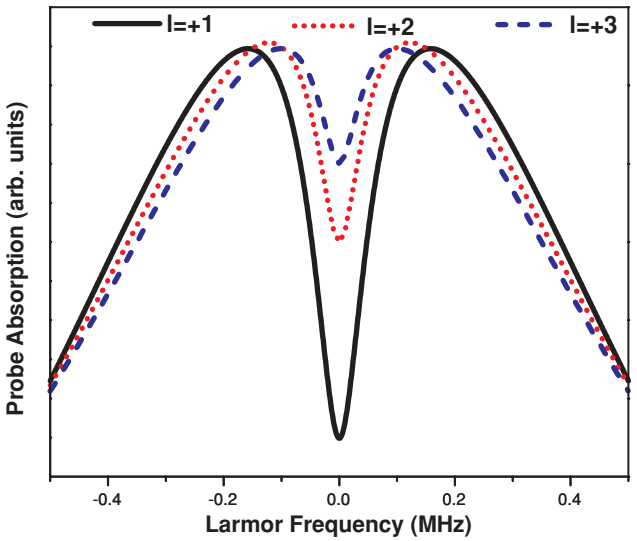

FIG. 5. (Color online) Probe absorption with the LG field for azimuthal mode indices, $l = +1, +2$, and $+3$ with w_o =2 mm, 3 mm, and 4 mm, respectively. Plotting style and other parameters are the same as those used in Fig. 2.

4 mm [26]. The EIT width decreases from 0.105 MHz for $l = 1$ to 0.084 MHz for $l = 2$ and 0.075 MHz for $l = 3$ (Fig. 5). LG-field-induced narrow EIT profiles may have several important applications such as atomic clocks and magnetometers with higher precision and increased storage times or steeper dispersion in stopped-light or slow-light experiments.

IV. EXPERIMENTAL DETAILS

An experimental study of the Hanle profile was carried out with Gaussian and LG fields to verify these results. Hanle measurements were carried out with Rb vapor with an external cavity diode laser locked to the $F_g = 2 \rightarrow F_e = 3$ transition of Rb^{87}. This transition gives rise to an EIA and has been studied by several groups [3,8,27]. The LG beam was created using a computer-generated hologram (CGH) [28]. The transmittance function of the CGH denoted by $T(r, \phi) = \exp[i\delta H(r, \phi)]$, is the Fourier transform of the interference pattern of a plane wave with an LG beam. Here, δ is the amplitude of the phase modulation. $H(r, \phi)$ defines the pattern of the CGH and is given by

$$H(r,\phi) = \frac{1}{2\pi} \bmod \left(l\phi - \frac{2\pi}{\Lambda} r \cos\phi, 2\pi \right), \qquad (12)$$

where Λ is the fringe spacing and $\bmod(a,b) = a - b\,\mathrm{int}(a/b)$.

The beam with azimuthal mode index $l = +1$ was used as the probe beam. The probe transmission was measured as a function of magnetic field scanned perpendicular to the direction of the probe beam along the x axis. The probe beam was polarized along the y axis (Fig. 6). The fields in the other two directions were reduced down to ~0.3 mG using Helmholtz coils. Measurements were also made with a Gaussian beam of the same intensity. Intensities of both the beams were fixed well below the saturation intensity.

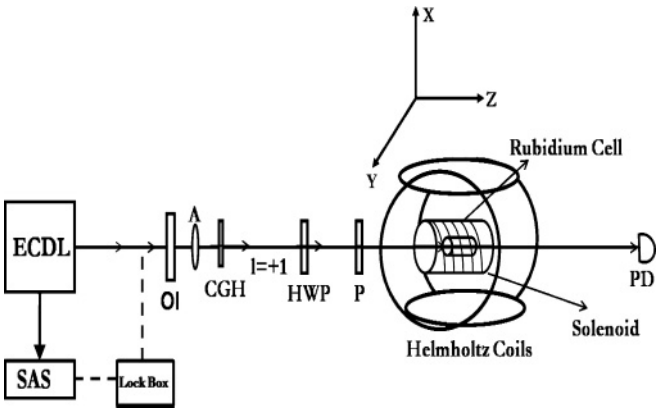

FIG. 6. Experimental setup used for measuring the Hanle profile with an LG beam, ECDL, external cavity diode laser; SAS, saturation absorption spectroscopy setup; OI, optical isolator; A, aperture; P, polarizer; CGH, computer-generated hologram; PD, photodetector; l, orbital angular momentum; HWP, half-wave plate.

The Hanle profile obtained with Gaussian and LG beams is shown in Fig. 7. The LG profile is distinctly narrower than the Gaussian beam profile confirming our computational results. The measured linewidths of the Hanle EIA profile for Gaussian and LG beams are 0.34 Gauss and 0.16 Gauss, respectively.

The influence of the LG beam on the Zeeman coherence was confirmed with a two-beam Hanle measurement. The Hanle profile was measured with a Gaussian beam in the presence of an LG beam ($l = +l$). Both beams were rendered circularly polarized, locked to the $F_g = 2 \rightarrow F_e = 3$ transition of Rb^{87} and co-propagated through the Rb vapor cell after which the LG beam was blocked and the transmission of the Gaussian beam at a power of 80 μW was measured. The LG beam (~2 μW) induces a noticeable (~50 mG) narrowing of the Hanle profile [Fig. 8(a)]. No narrowing is observed when the

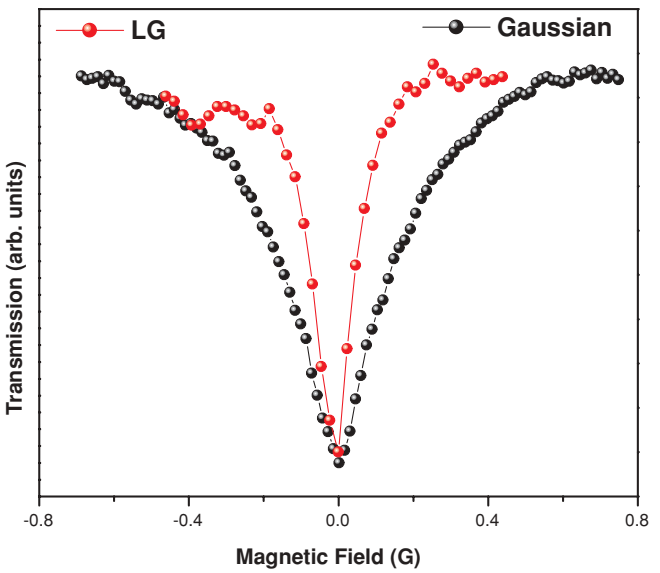

FIG. 7. (Color online) Measured Hanle EIA profiles for Gaussian and LG beams locked to the $F_g = 2 \rightarrow F_e = 3$ transition of Rb^{87}. The probe power was 53 μW for both beams.

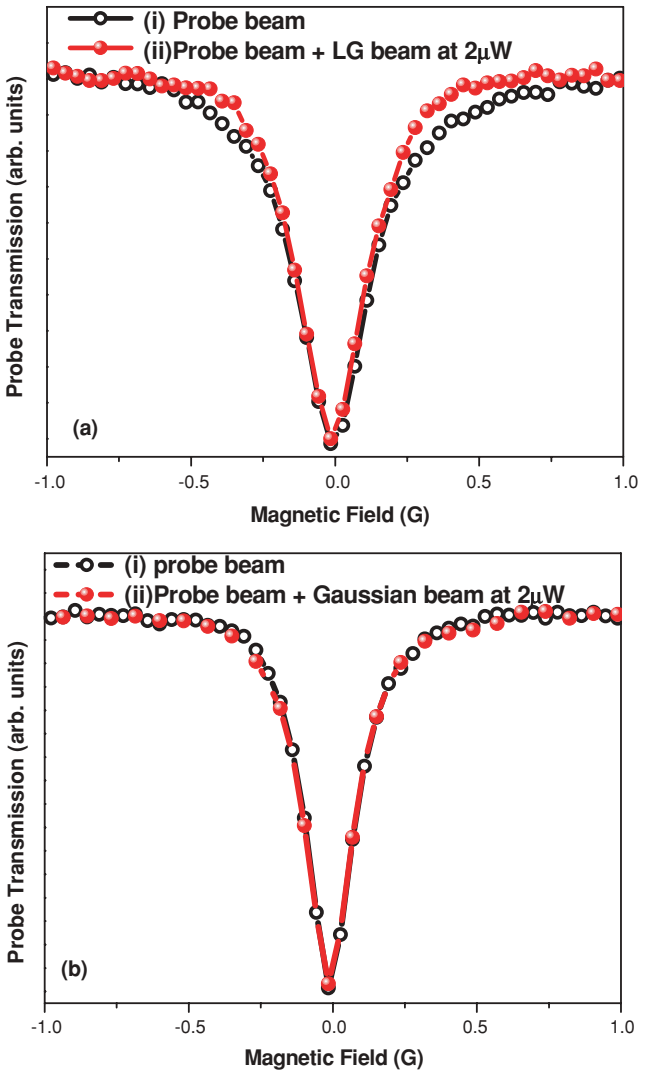

FIG. 8. (Color online) Measured Hanle EIA profile for Gaussian beam (80 μW) locked to the $F_g = 2 \rightarrow F_e = 3$ transition of Rb^{87} with and without a coupling beam. The coupling beam is (a) LG and (b) Gaussian. Introduction of the LG beam lowers the linewidth of the Gaussian EIA Hanle profile from 0.31 Gauss to 0.26 Gauss.

LG beam is replaced with a Gaussian beam ($l = 0$) [Fig. 8(b)]. The observed narrowing suggests that the presence of the LG beam enhances the lifetime of the Zeeman coherences probed by the Gaussian beam in further support of our computational analysis.

The difference in linewidth between the Hanle EIA profile of a pure Gaussian beam and that of the Gaussian beam in the presence of a LG beam ($\Delta_G - \Delta_{G/\mathrm{LG}}$) is plotted in Fig. 9 as a function of the LG beam power. With increase in the power of the LG beam, ($\Delta_G - \Delta_{G/\mathrm{LG}}$) decreases. When the LG beam power exceeds 98 μW, the power corresponding to the saturation intensity, power broadening dominates, and ($\Delta_G - \Delta_{G/\mathrm{LG}}$) becomes negative. Thus, the influence of the azimuthal mode index on the Zeeman coherence lifetime depends on the intensity of the LG field.

Strong experimental support to our results is found by comparing degenerate four-wave mixing experiments [29]

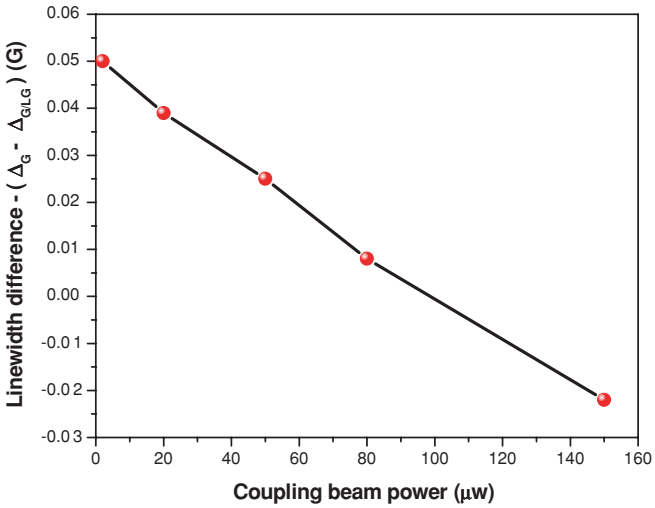

FIG. 9. (Color online) Difference in linewidth between the Hanle EIA profile of a pure Gaussian beam and that of the Gaussian beam in the presence of an LG beam ($\Delta_G - \Delta_{G/\mathrm{LG}}$) for different powers of the LG beam. Both beams were locked to the $F_g = 2 \rightarrow F_e = 3$ transition of Rb^{87} and the Gaussian beam power was fixed at 80 μW.

performed with the Gaussian [30] and LG [31] signal beams. All other experimental conditions being the same, the sub-natural four-wave mixing spectral linewidth obtained with a Gaussian signal beam was found to be approximately 187 KHz [32] higher than the 200-KHz linewidth obtained with an LG signal beam [31]. Since the four-wave mixing spectrum originates from a long-lived Zeeman ground-state coherence [31], the use of an LG beam is found to enhance the Zeeman coherence lifetime in agreement with the present results. Further support is obtained when experiments on the topological study of stored optical vortices are considered [33]. An LG mode (optical vortex) could be stored in hot atomic vapor for 110 μs without diffusion while the corresponding time for a Gaussian beam with a uniform phase and a dark center was found to be only 10 μs. Since the storage time is directly proportional to the lifetime of ground-state coherences [34,35], the study confirms that a nonzero azimuthal mode index is crucial to producing long-lived ground-state coherences and hence enhanced storage times.

In conclusion, the influence of a Laguerre Gaussian beam on the linewidth of electromagnetically induced Hanle EIT and EIA profiles has been studied. We have shown by computation and experiment that the azimuthal mode index of the LG field induces long-lived Zeeman coherences resulting in a significant narrowing of the Hanle EIT and EIA resonance. LG-field-induced narrowing of EIT and EIA profiles may have several important applications such as atomic clocks, magnetometers, slow light, etc. Additional experiments on coherence-induced phenomenon using spatially varying optical fields are in progress.

ACKNOWLEDGMENTS

The authors thank Mr. Senthil Kumar for fabricating the computer generated hologram that was used to create the Laguerre Gaussian beam. This work was supported by the Department of Science and Technology, India.

[1] H. R. Gray, R. M. Whitley, and C. R. Stroud, Opt. Lett. **3**, 218 (1978).
[2] H. Steve, Phys. Today **50**, 36 (1997).
[3] F. Renzoni, C. Zimmermann, P. Verkerk, and E. Arimondo, J. Opt. B: Quantum Semiclass. Opt. **3**, S7 (2001).
[4] M. Fleischhauer, A. Imamoglu, and J. P. Marangos, Rev. Mod. Phys. **77**, 633 (2005).
[5] E. Arimondo, *Progress in Optics*, edited by E. Wolf (Elsevier, Amsterdam, 1996), Vol. XXXV, p. 257; J. P. Marangos, J. Mod. Opt. **45**, 471 (1998).
[6] A. Lezama, S. Barreiro, and A. M. Akulshin, Phys. Rev. A **59**, 4732 (1999).
[7] A. V. Taichenachev, A. M. Tumaikin, and V. I. Yudin, Phys. Rev. A **61**, 011802(R) (1999).
[8] Y. Dancheva, G. Alzetta, S. Cartaleva, M. Taslakov, and Ch. Andreeva, Opt. Commum. **178**, 103 (2000).
[9] A. Corney, *Atomic and Laser Spectroscopy* (Oxford University Press, Oxford, 1977).
[10] M. E. J. Friese, J. Enger, H. Rubinsztein-Dunlop, and N. R. Heckenberg, Phys. Rev. A **54**, 1593 (1996).
[11] L. Allen, M. Babiker, W. K. Lai, and V. E. Lembessis, Phys. Rev. A **54**, 4259 (1996).
[12] J. W. R. Tabosa and D. V. Petrov, Phys. Rev. Lett. **83**, 4967 (1999).
[13] J. Courtial, K. Dholakia, L. Allen, and M. J. Padgett, Phys. Rev. A **56**, 4193 (1997).
[14] L. Allen, M. Babiker, and W. L. Power, Opt. Commun. **112**, 141 (1994).
[15] S. Barreiro, J. W. R. Tabosa, H. Failache, and A. Lezama, Phys. Rev. Lett. **97**, 113601 (2006).
[16] I. V. Basistiy, V. V. Slyusar, M. S. Soskin, M. V. Vasnetsov, and A. Ya. Bekshaev, Opt. Lett. **28**, 1185 (2003).
[17] V. E. Lembessis, Opt. Commun. **159**, 243 (1999).
[18] W. L. Power, L. Allen, M. Babiker, and V. E. Lembessis, Phys. Rev. A **52**, 479 (1995).
[19] F. Renzoni, W. Maichen, L. Windholz, and E. Arimondo, Phys. Rev. A **55**, 3710 (1997).
[20] B. H. Bransden and C. J. Joachain, *Physics of Atoms and Molecules*, 2nd ed. (Pearson Education, Upper Saddle River, 2004).
[21] M. O. Scully and M. S. Zubairy, *Quantum Optics* (Cambridge University Press, Cambridge, 1997).
[22] R. Loudon, *The Quantum Theory of Light* (Oxford University Press, Oxford, 1983).
[23] Computed with a user-extensible mathematics-based atomic density matrix package, ATOMICDENSITYMATRIX, by Simon Rochester; available online at http://budker.berkeley.edu/ADM.
[24] R. W. Boyd, *Nonlinear Optics*, 2nd ed. (Academic, San Diego, 2003).
[25] R. J. McLeant, R. J. Ballagh, and D. M. Warrington, J. Phys. B: At. Mol. Phys. **18**, 2371 (1985).
[26] V. V. Kotlyar, S. N. Khonina, A. A. Kovalev, V. A. Soifer, H. Elfstrom, and J. Turunen, Opt. Lett. **31**, 1597 (2006); Have shown that the LG beam waist increases with increase in l. Values of 3 and 4 mm for $l = 2$ and 3 were chosen to represent this feature ($w_0 = 2$ mm for $l = 1$; was obtained from the computer-generated hologram). Results of Fig. 5 remain unchanged if the same w_0 (=2 mm) is used for $l = 2$ and 3.
[27] J. Dimitrijević, A. Krmpot, M. Mijailović, D. Arsenović, B. Panić, Z. Grujić, and B. M. Jelenković, Phys. Rev. A **77**, 013814 (2008).
[28] H. He, N. R. Heckenberg, and H. Rubinsztein- Dunlop, J. Mod. Opt. **42**, 217 (1995).
[29] A good introduction to degenerate four-wave mixing can be found at J. F. Lam and R. L. Abrams, Phys. Rev. A **26**, 1539 (1982).
[30] A. Lezama, G. C. Cardoso, and J. W. R. Tabosa, Phys. Rev. A **63**, 013805 (2000).
[31] S. Barreiro and J. W. R. Tabosa, Phys. Rev. Lett. **90**, 133001 (2003).
[32] Line width from Ref. [30] was estimated by digitizing the reported data.
[33] R. Pugatch, M. Shuker, O. Firstenberg, A. Ron, and N. Davidson, Phys. Rev. Lett. **98**, 203601 (2007).
[34] Z. Dutton and J. Ruostekoski, Phys. Rev. Lett. **93**, 193602 (2004).
[35] J. W. R. Tabosa and A. Lezama, J. Phys. B: At. Mol. Opt. Phys. **40**, 2809 (2007).